Neuron, Volume *81*

Supplemental Information

NMDA Receptor-Dependent Multidendrite Ca^{2+} Spikes Required for Hippocampal Burst Firing In Vivo

Christine Grienberger, Xiaowei Chen, and Arthur Konnerth

SUPPLEMENTAL FIGURES AND LEGENDS

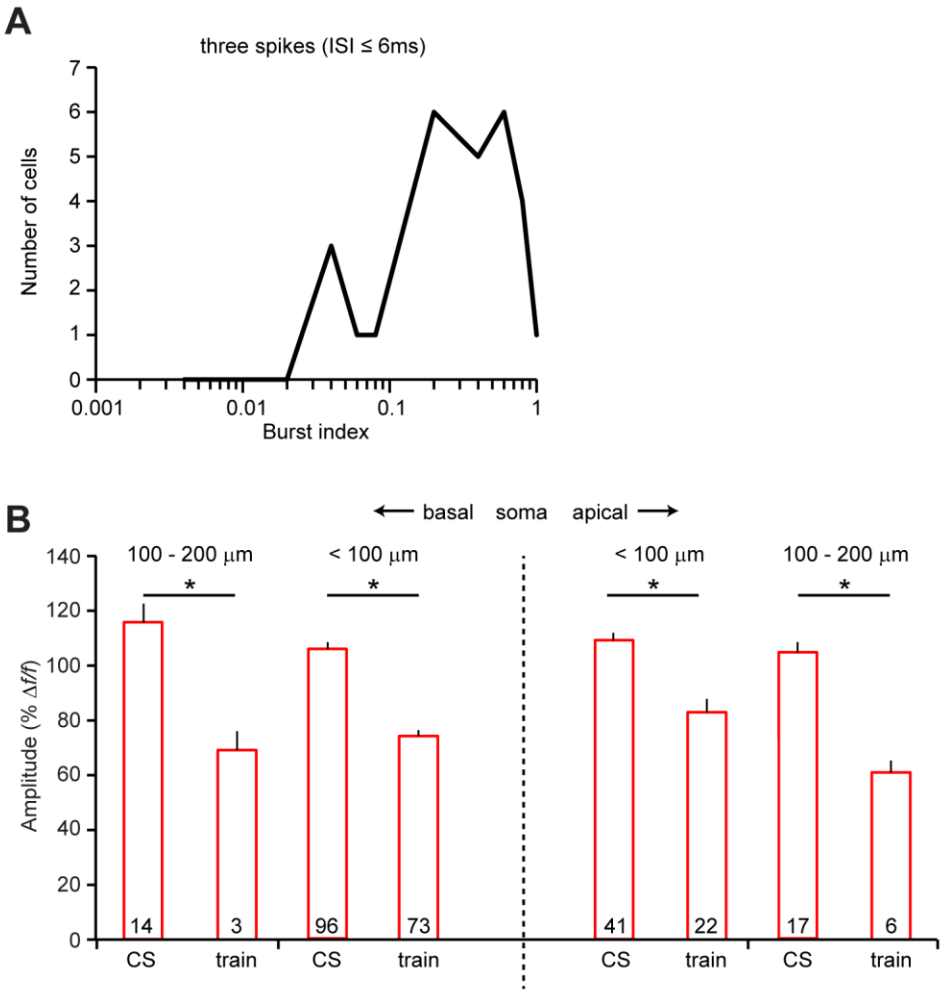

Figure S1. *In vivo* whole-cell recordings and dendritic Ca^{2+} signals in visually-identified CA1 pyramidal neurons. Related to Figure 1.

(A) Histogram showing the distribution of burst indices (number of spikes in bursts divided by all spikes) in CA1 pyramidal neurons. Note that here bursts are defined as series of three or more APs with ≤ 6 ms interspike interval. (B) Bar graph showing the amplitudes of dendritic Ca^{2+} signals, evoked by complex spike bursts and trains (without depolarizing wave) of APs in basal and apical dendrites. Shown is combined data of trains and CSs with 4 and 5 APs (mean±SEM, in % $\Delta f/f$, n=13 cells, Kolmogorov-Smirnov test, basal: <100 µm *p<0.001 and 100-200 µm *p<0.05, apical: <100 µm *p<0.001 and 100-200 µm *p<0.001). Note that since the number of dendritic branches (n) contributing to each data point varied the actual n values are indicated by small numbers.

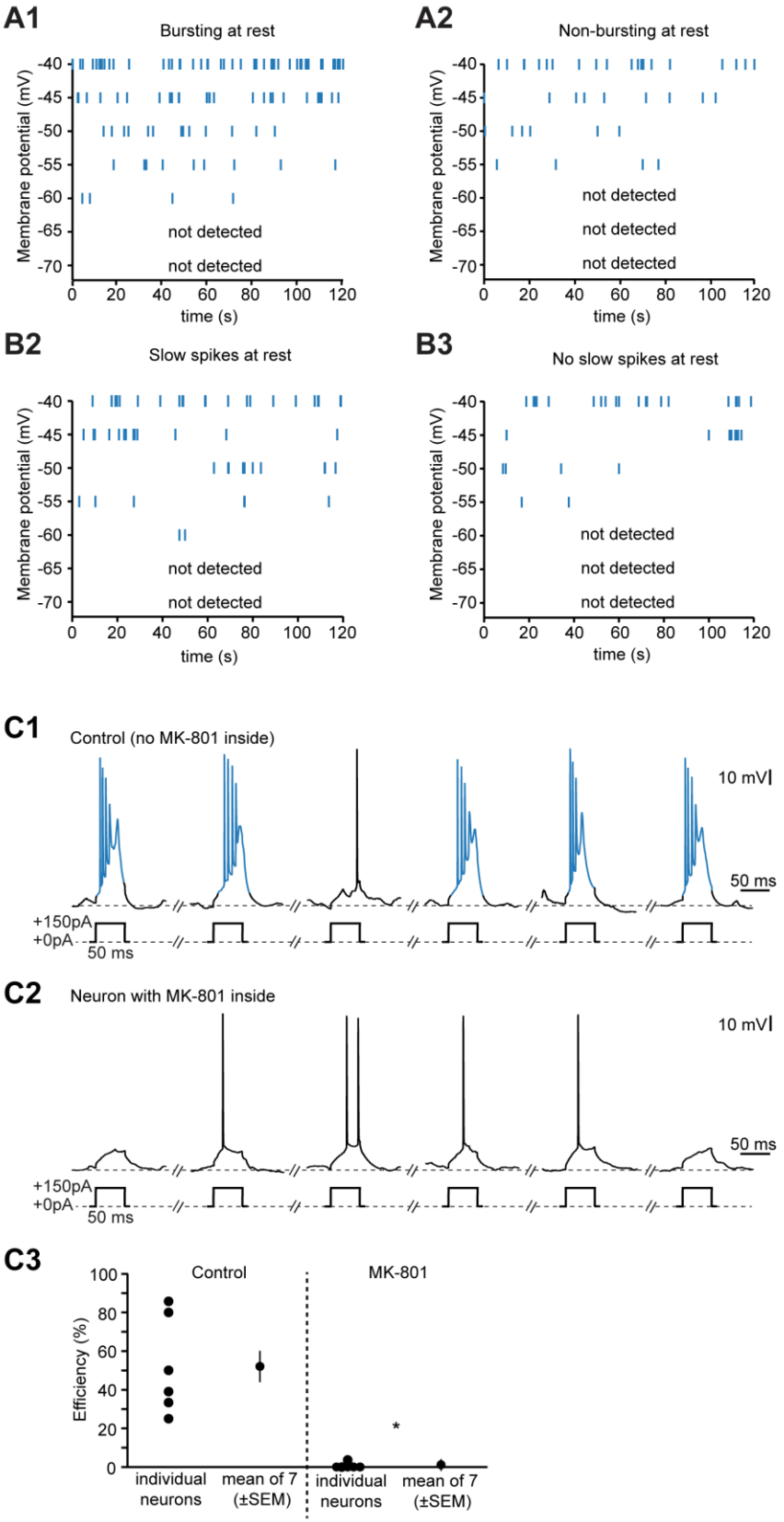
A1
Bursting at rest
Membrane potential (mV)
-40
-45
-50
-55
-60
-65
-70
not detected
not detected
0 20 40 60 80 100 120
time (s)
A2
Non-bursting at rest
Membrane potential (mV)
not detected
not detected
not detected
time (s)
B2
Slow spikes at rest
Membrane potential (mV)
not detected
not detected
time (s)
B3
No slow spikes at rest
Membrane potential (mV)
not detected
not detected
not detected
time (s)
C1
Control (no MK-801 inside)
10 mV
50 ms
+150pA
+0pA
50 ms
C2
Neuron with MK-801 inside
10 mV
50 ms
+150pA
+0pA
50 ms
C3
Control
MK-801
Efficiency (%)
100
80
60
40
20
0
*
individual neurons
mean of 7 (±SEM)
individual neurons
mean of 7 (±SEM)

Figure S2. Voltage-dependence of complex spike bursts and slow spikes. Related to Figures 2 and 3.

(A-B) Raster plots showing the distribution of CSs (A) and slow spikes (B) in four different neurons. Please note the stochastic nature of burst (A) and slow spike (B) patterns at all membrane potentials tested. (C) Short current pulses can evoke complex spike bursts. (C1) Responses to depolarizing current pulses (50 ms, 150 pA) under control conditions. (C2) Responses to depolarizing current pulses (50 ms, 150 pA) in the presence of MK-801. (C3) Efficiency to evoke CSs using depolarizing current pulses under control conditions (left) or with MK-801 inside (right). The stimulus efficiency was calculated as the fraction of current pulses (n=10-40) evoking a CS. (n=7 neurons, Kolmogorov-Smirnov test, *$p<0.005$).

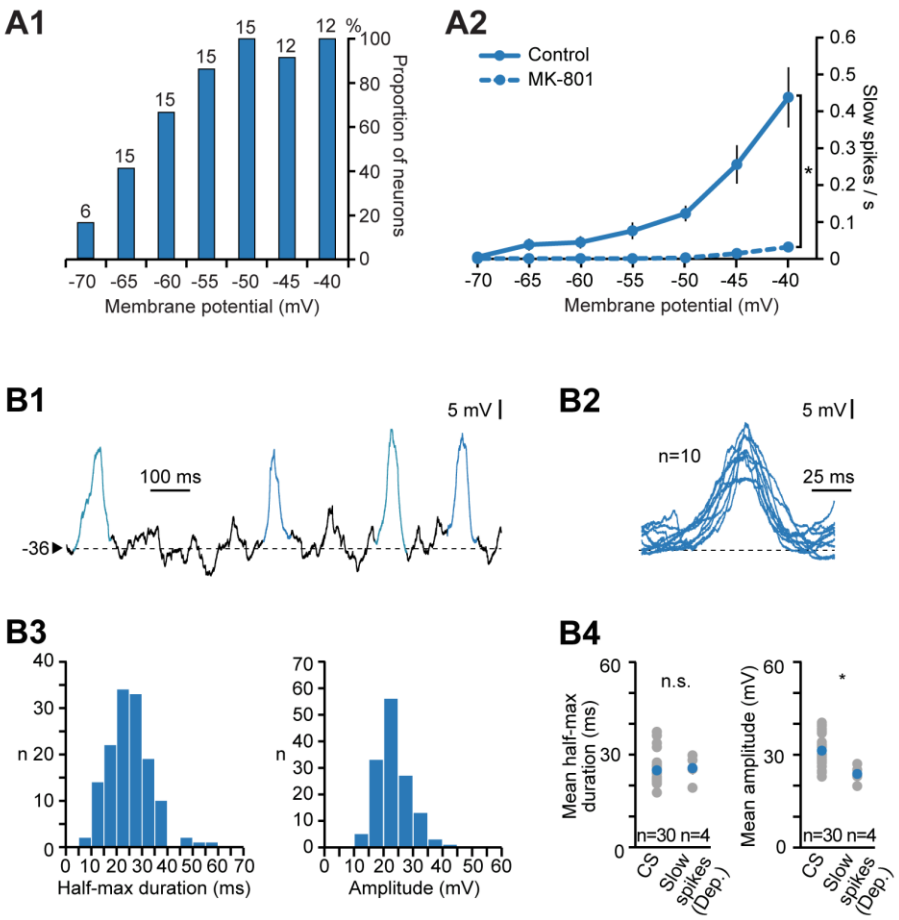

Figure S3. Properties of slow spikes. Related to Figure 3.
(A1) Proportion of neurons (with QX-314 inside) exhibiting slow spikes. Note that since the number of experiments (n) contributing to each data point varied the actual n values are indicated by the small numbers next to the bars. (A2) Slow spike frequency in neurons in the presence of QX-314 (control) or in the presence of QX-314 and MK-801 (n=18 and 5 neurons, Kolmogorov-Smirnov test, -55 mV *p<0.05, -50 mV *p<0.005, -45 mV *p<0.05, -40 mV *p<0.005). (B) Depolarization-mediated block of action potentials reveals slow spike-like potentials. (B1) Spontaneous activity at a membrane potential of –36 mV. (B2) Overlay of 10 consecutive slow spike-like potentials, recorded at depolarized membrane potential. (B3) Histograms showing the distribution of the half-max durations (left panel) and the amplitudes (right) of the slow spike-like potentials (n=138 from 4 neurons). (B4) Comparison of the half-max durations (left panel) and amplitudes (right panels) of CSs and slow spike-like potentials. Shown are data points from individual animals (grey) and the mean values ± SEM. (Half-max duration: 25±1 ms and 25 ± 2 ms, Mann-Whitney test, p=0.572; Amplitude: 31±1 mV and 23±1 mV, Mann-Whitney test, p<0.01).

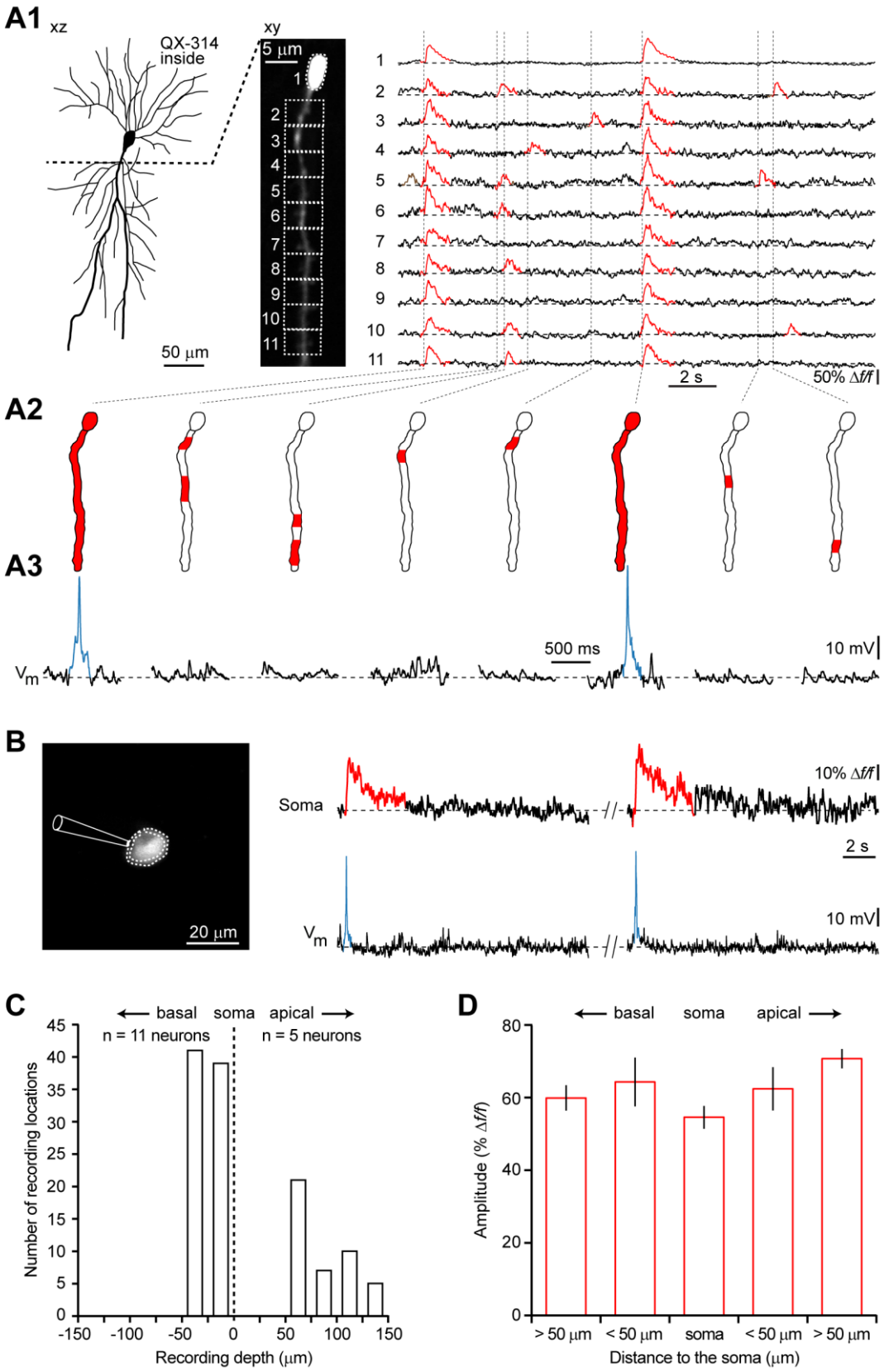
A1
xz
QX-314
inside
50 µm
xy
5 µm
1
2
3
4
5
6
7
8
9
10
11
2 s
50% Δf/f
A2
A3
500 ms
10 mV
Vm
B
20 µm
Soma
10% Δf/f
2 s
10 mV
Vm
C
basal
soma
apical
n = 11 neurons
n = 5 neurons
Number of recording locations
Recording depth (µm)
D
basal
soma
apical
Amplitude (% Δf/f)
> 50 µm
< 50 µm
soma
< 50 µm
> 50 µm
Distance to the soma (µm)

Figure S4. Ca^{2+} spikes in different cellular compartments. Related to Figure 4.
(A1) Left panel: post-hoc reconstruction of a biocytin-filled neuron. Dotted line indicates plane of focus used for imaging spontaneous Ca^{2+} transients in the ROIs 1-11 in the presence of QX-314 (right panel). ROIs (3x4 μm size) are indicated on the fluorescent image (middle panel). (A2-3) Corresponding Ca^{2+} signals (A2, red) and membrane potential recording (A3, slow spikes in blue) (B) Left panel: two-photon image of the cell soma (with QX-314 inside). Right panel: Corresponding Ca^{2+} signals (red) and membrane potential recording (slow spikes in blue). (C) Histogram showing the distribution of the depths of recording locations in reference to the cell soma layer. (D) Bar graph showing the amplitude of 'global' dendritic Ca^{2+} signals (mean±SEM, in % $\Delta f/f$). Fluorescent images are averages of 1200 frames.

SUPPLEMENTAL EXPERIMENTAL PROCEDURES

Animals and surgery. All experimental procedures were performed in accordance with institutional animal welfare guidelines and were approved by the state government of Bavaria, Germany. C57BL/6 mice (p28-65, n=27) were used for *in vivo* whole-cell patch clamp recordings and recordings of dendritic Ca^{2+} signals. Surgery was carried out as described previously (Jia et al., 2010). In brief, the mouse was placed onto a warming plate (37.5-38°C) and anesthetized by inhalation of 1.3-1.5% isoflurane (Abbott, Germany) in pure O_2. The depth of anesthesia was assessed by monitoring the tail-pinch reflex and the respiratory activity. The eyes were protected by application of Isopto-max crème (Alcon Pharma, Germany). The skin was removed under a dissection microscope after locally applying an anesthetic agent (Xylocaine, AstraZeneca, Germany). A custom-made recording chamber was glued to the skull with cyanoacrylic glue (UHU, Germany). The stereotactic coordinates of the hippocampus were located using a mouse brain atlas (Paxinos and Franklin, 2001). A dental drill and a thin (30 G) injection needle were then used to open a 1-2 mm-wide cranial window in the skull centered 2.6 mm posterior to bregma and 2.3 mm lateral to the midline. The dura was dissected with a fine forceps and a small part of the cortical tissue that covered the hippocampal surface was carefully removed by aspiration (Busche et al., 2012; Dombeck et al., 2010; Mizrahi et al., 2004). Then the dorsal surface of the hippocampus was rinsed with warm (37°C) external saline and covered with 2% low-melting-point agarose to increase mechanical stability (~1.5-mm thick). After surgery, the mouse was transferred into the recording apparatus and recordings were performed under light levels of anesthesia (0.7-0.8% of isoflurane in O_2; e.g. breathing rate of ~120-140 breaths per minute). The recording chamber was perfused with warm normal Ringer's solution containing: (in mM) 125 NaCl, 4.5 KCl, 26 $NaHCO_3$, 1.25 NaH_2PO_4, 2 $CaCl_2$, 1 $MgCl_2$ and 20 glucose (pH 7.4 when bubbled with 95% O_2 and 5% CO_2). The temperature of the mouse was maintained at values between 37°C and 37.5°C by using a heating plate.

***In vivo* electrophysiology.** Somatic whole-cell patch-clamp recordings of CA1 pyramidal neurons (cell bodies ~120-200 μm from the hippocampal surface) were obtained with an EPC-9 amplifier (HEKA Elektronik, Germany) by using the 'shadow patching' procedure(Kitamura et al., 2008). Borosilicate glass patch pipettes (Hilgenberg GmbH, Germany) with open-tip resistances of 5–7 MΩ were filled with a pipette solution containing 135 mM K-gluconate, 10 mM HEPES, 10 mM Na_2-phosphocreatine, 4 mM KCl, 4 mM MgATP, 0.3 mM Na_3GTP, 100-150 μM Oregon Green BAPTA-1 hexapotassium salt (OGB-1; Invitrogen) and 25-50 μM Alexa Fluor 594 hydrazide sodium salt (Alexa-594). In some recordings, the pipette solution contained biocytin 0.2% for post-hoc morphological verification. For pharmacological experiments, 1 mM MK-801 (a use-dependent, non-competitive NMDA receptor antagonist), 0.5-3 mM QX-314 (a blocker of predominantly voltage-gated Na^+ channels) or 1-5 mM D-890 (a broad-range blocker of voltage-gated Ca^{2+} channels) was added to the pipette solution. Recordings were usually started 2-5 minutes after establishing the whole-cell configuration. As exception, recordings in neurons with MK-801 application from the inside were started earlier in order to obtain control recordings. Neurons were only used for recording if the series resistance was below 50 MΩ. Electrophysiological

data were filtered at 3 kHz and sampled at 20 kHz using the Pulse software (HEKA Elektronik, Germany). The mean resting membrane potentials (not corrected for the liquid junction potential) was -61 ± 0.9 mV (mean ± SEM). To determine the relationship between membrane potential and CS frequency, neurons were depolarized by sustained current injections through the recording pipette. Spontaneous activity at the different membrane potential levels (resting state and depolarized state) was recorded for 2 min. The following membrane potential values (in mV) were included: -70 (-72 to -68), -65 (-67 to -63), -60 (-62 to -58), -55 (-57 to -53), -50 (-52 to -48), -45 (-47 to -43), -40 (-42 to -38). Similarly, depolarization through sustained current injection was used to induce the depolarization-mediated block of APs. Whole-cell recordings were targeted to excitatory pyramidal neurons in the CA1 region of the hippocampus, based on the following criteria: (1) stereotaxic coordinates (Paxinos and Franklin, 2001), (2) cell body located within the stratum pyramidale, and (3) presence of apical and basal spiny dendrites that extended from the conical soma (Megias et al., 2001).

High-speed two-photon Ca^{2+} imaging. In a subset of neurons (n=39 neurons), in parallel to somatic membrane potential recordings, *in vivo* Ca^{2+} imaging was performed using a custom-built two-photon microscope. A resonant scanner unit (GSI Lumonics, Germany), including one fast axis of a 12 kHz resonant mirror and one slow axis of a standard galvanometric mirror, was mounted on an upright microscope chassis (BX51; Olympus, Japan) with a long working distance water-immersion objective (40×/0.8NA, 3.5 mm WD; Nikon, Japan)(Varga et al., 2011). Fluorescent excitation light was delivered by a pulsing infrared laser (wavelength=800 or 925 nm, pulse width=100 fs, repetition rate=80 MHz) equipped with a prechirper (model Mai-Tai DeepSee; Spectra-Physics, USA). Emitted photons were detected by two detection channels equipped with photomultiplier tubes (H7424-40; Hamamatsu, Japan), a 'green' channel for OGB-1-dependent Ca^{2+} recordings (480-560 nm) and a 'red' channel for the Alexa-594 fluorescence (580-680 nm). The laser scanning and image acquisition were controlled by a real-time PXI computer (PXIe-1082; National Instruments) equipped with FPGA I/O board (PXI-7831R) and high-speed digitizer (PXI-5122). For dendritic imaging, full-frame images were acquired at 40 Hz (512x512 pixels) or 80 Hz (512x256 pixels) using a custom-programmed software based on LabVIEW™ (version 2009; National Instruments, USA). The laser power under the objective was typically between 15-30 mW. Ca^{2+} imaging was started approximately 10 min after establishing the whole-cell configuration, to allow the diffusion of the Ca^{2+} dye and/or of pharmacological agents into the dendrites. At this time point the dendrites of the CA1 pyramidal neurons were well labeled by OGB-1 and Alexa-594. The focal plane was chosen to contain as many dendrites as possible (up to about 150 μm below the cell somata, see e.g. Figure S4C). At each focal plane, we imaged spontaneous dendritic Ca^{2+} transients for at least 2 min. At the end of each experiment, a z-stack of the fluorescently labeled neuron was acquired (512x512 pixels, 270x270 μm field of view, 0.5 μm step size).

External drug application. In some experiments, a second glass pipette filled with 500 μM d-APV (D-2-amino-5-phosphonovaleric acid) and 10 μM Alexa-594, diluted in standard extracellular saline solution, was placed under two-photon guidance close the neuron of interest. The drug was delivered by gentle

pressure injection. The area of diffusion was monitored at the beginning of each recording trial by imaging the Alexa-594 fluorescence.

Data analysis. All the analyses were restricted to excitatory neurons that were identified according to the previously-described criteria, assessed after the experiment in either the post-hoc reconstructions of biocytin-filled neurons and/or the reconstructions of *in vivo* z-stacks of the recorded neurons (see Figure 1). Electrophysiology and Ca^{2+} imaging data were analyzed off-line by using custom-written procedures in Igor Pro™ (Wavemetrics, USA) and LabVIEW™ (version 2009, National Instruments, USA)(Jia et al., 2011). The depolarizing wave associated with complex spike bursts was determined by interpolating the inter-spike minima. After background subtraction relative changes in the Ca^{2+}-dependent fluorescence ($\Delta f/f$) represent the mean fluorescence changes of all pixels within specified region of interests (ROIs). Their sizes varied between ROIs comprising the whole dendritic branch to smaller ROIs of 3x4 μm. Ca^{2+} transients were automatically detected with a template-matching algorithm, taking into account the rise and decay times properties of the Ca^{2+} signals. A Ca^{2+} transient was accepted as a signal when its amplitude was greater than 3 times the standard deviation of the noise band. To improve the visibility of Ca^{2+} transients, the $\Delta f/f$-traces shown in all figures were smoothed with an exponentially averaging IIR filter (time constant 50 ms)(Jia et al., 2010). The top view and side view reconstructions of recorded neurons were generated from the individual z-stack images from the red Alexa-594 channel of the two-photon microscope. The reconstructed images were obtained using Image J (free online access at: http://rsbweb.nih.gov/ij/). The z-stack images were also used to measure the distance of the dendritic branches to the soma.

Burst index. For the analysis in Figure S1A a burst was defined as a series of at least three spikes with ≤ 6 ms interspike interval. The burst index represents the number of spikes in bursts divided by all spikes.

Statistical analysis. Statistical analyses were performed using the SPSS software (version 21.0, IBM, USA), applying the non-parametric Mann-Whitney and Kolmogorov-Smirnov tests, as indicated in the figure legends. $P<0.05$ was considered statistically significant.